

Two photon decays of heavy vector mesons $B^* \rightarrow B \gamma \gamma$, $D^* \rightarrow D \gamma \gamma$, and the possible determination of the $g_{B^*(D^*)B(D)\pi}$ and $g_{B^*0B^0\gamma}$ couplings

Dafne Guetta* and Paul Singer†

Department of Physics, Technion- Israel Institute of Technology, Haifa 32000, Israel

(Received 26 April 1999; revised manuscript received 9 September 1999; published 10 February 2000)

We study the novel decays $B^* \rightarrow B \gamma \gamma$ and $D^* \rightarrow D \gamma \gamma$ using the framework of the heavy meson chiral Lagrangian (HM χ L) to leading order in chiral perturbation theory. The branching ratios of these decays are expressed in terms of the strong $g_{B^*(D^*)B(D)\pi}$ and the electromagnetic $g_{B^*(D^*)B(D)\gamma}$ couplings, thus providing a possible tool for their determination. In the charm case, using the experimentally determined ratios $(D^{*0,+} \rightarrow D\pi)/(D^{*0,+} \rightarrow D\gamma)$, we are able to express the branching ratio as a function of the strong coupling only. We thus find $1.6 \times 10^{-6} < \text{Br}(D^{*0} \rightarrow D^0 \gamma \gamma) < 3.3 \times 10^{-5}$ for $0.25 < g < 1$, where g is the strong coupling of HM χ L. In the b -flavored sector, the $\text{Br}(B^{*0} \rightarrow B^0 \gamma \gamma)$ which we estimate to be in the $10^{-7} - 10^{-5}$ range is a function of both $g_{B^*B\pi}$ and $g_{B^*B\gamma}$. Its behavior does not afford an unambiguous determination of these couplings except for the region of high g values such as $g > 0.6$. The expected two-photon differential distributions are presented for both $B^{*0} \rightarrow B^0 \gamma \gamma$ and $D^{*0} \rightarrow D^0 \gamma \gamma$, for different values of the couplings involved.

PACS number(s): 12.39.Fe, 12.39.Hg, 13.20.He

I. INTRODUCTION

The heavy vector mesons B^* and D^* (of spin-parity 1^-) decay via spin-flip electromagnetic or strong interactions to the well-studied pseudoscalar ground states B and D . The decays of D^* are known to proceed either as a strong transition $D^* \rightarrow D\pi$ with a final pion with momentum of about 40 MeV or as an electromagnetic one $D^* \rightarrow D\gamma$, with a final photon with momentum of about 140 MeV. The situation is different for B^* which has a mass of 5324.9 ± 1.8 MeV; since the mass difference $M_{B^*} - M_B$ is only 45.8 MeV, there is no strong B^* decay and the radiative process $B^* \rightarrow B\gamma$ is the dominant decay mode for B^* .

In the present paper we study another possible electromagnetic decay, the two-photon decay processes $B^* \rightarrow B\gamma\gamma$ and $D^* \rightarrow D\gamma\gamma$ which were not considered previously in the literature. In addition to the intrinsic interest in these novel modes, we point out that their study could provide information on the strong couplings $g_{B^*B\pi}$ and $g_{D^*D\pi}$ and on the electromagnetic ones $g_{B^*B\gamma}$, $g_{D^*D\gamma}$. The strong couplings are directly related to the basic strong coupling g of the effective heavy meson chiral Lagrangian, which describes the interactions of heavy mesons with low-momentum pions.

There is a major dissimilarity between the possibility of measuring the couplings in the charm and b -flavored sectors, as a result of the different mass difference between the respective vector and pseudoscalar mesons. In the charm sector, the experimentally measured branching ratios of the D^{*0}, D^{*+} decays into the allowed $D\pi$ and $D\gamma$ modes lead to relations between $g_{D^*D\pi}$ and $g_{D^*D\gamma}$. Henceforth, the $D^* \rightarrow D\gamma\gamma$ decay under study here is expressible in terms of the strong coupling only and would provide a convenient tool for its measurement.

On the other hand, in the b -flavored sector where the $B^* \rightarrow B\pi$ decay is forbidden by phase space, the $g_{B^*B\pi}$ coupling is not directly accessible. And although the $B^* \rightarrow B\gamma$ decay is experimentally detected, the direct measurement of its strength is an unlikely proposition at present, in view of the smallness of the expected value of its decay width.

However, as we show in this paper, the two photon decay $B^* \rightarrow B\gamma\gamma$ branching ratio turns out to be a function of $g_{B^*B\pi}$ and $g_{B^*B\gamma}$, which opens the possibility for their determination, especially in particularly favorable regions of the $[g_{B^*B\pi}, g_{B^*B\gamma}]$ parameter space.

Our analysis singles out the neutral modes $B^{*0}(D^{*0}) \rightarrow B^0(D^0)\gamma\gamma$ as the more relevant ones in relation with the determination of the the couplings under consideration. In addition to the direct radiative transition which is the sole contribution in neutral decays, and on which we concentrate in this paper, there is also the two-photon decay arising from bremsstrahlung in the charged $B^{*+}(D^{*+}) \rightarrow B^+(D^+)\gamma$ channel. Since this radiation overwhelms the direct mode, as we will show, one has to resort to the investigation of the neutral modes if one aims for a cleaner determination of the strong couplings.

In Sec. II we review the present status of the main decays of B^* and D^* , with which the rare two photon decays must be compared. In Sec. III we present the theoretical framework of our approach. Section IV contains the explicit treatment of the decay amplitudes. In the last section we summarize our predictions and we discuss certain features of the calculation.

II. EXPERIMENTAL AND THEORETICAL STATUS OF B^* AND D^* PRINCIPAL DECAYS

The vector mesons B^* were firstly observed [1] by the CUSB Collaboration at the Cornell Electron Storage Ring (CESR) by detecting the photon signal from the radiative decay $B^* \rightarrow B\gamma$. This signal of 46 MeV photons was confirmed in improved CUSB-II measurements, with the vector

*Email address: firenze@physics.technion.ac.il

†Email address: phr26ps@physics.technion.ac.il

mesons produced at CESR at the $Y(5S)$ resonance [2]. Recently the process $B^* \rightarrow B\gamma$ has been observed also at the CERN e^+e^- collider LEP with the various detectors [3] in a sample of over 4×10^6 hadronic Z^0 decays. The rate of the B^* -meson production relative to that of B mesons is found generally to be consistent with the expectation from spin counting. It is expected that this production rate will be maintained in future B experiments at hadron machines, such as the BTeV at Fermilab and Large Hadron Collider (LHC) at CERN, where samples of the order of 10^{10} B^* 's are expected. Then, a fairly high sensitivity can be achieved in the study of B^* decays and measurements of B^* branching ratios of the order 10^{-7} – 10^{-8} could be accessible.

In view of the small mass difference $\Delta M(B^* - B) = 45.78 \pm 0.35$ MeV [4], which forbids strong B^* decays, the electromagnetic transition $B^* \rightarrow B\gamma$ appears as the main decay of B^* . This decay has been studied in a variety of theoretical models, including quark models [5–7], the chiral bag model [8] followed by effective chiral Lagrangian approaches for heavy and light mesons [9–11], potential models [12,13] and QCD sum rules [14,15]. The predictions of these calculations span a range of nearly one order of magnitude for the expected decay widths, between $\Gamma(B^{*0}(B^{*+}) \rightarrow B^0(B^+)\gamma) = 0.04(0.10)$ keV [14] and $\Gamma(B^{*0}(B^{*+}) \rightarrow B^0(B^+)\gamma) = 0.28(0.62)$ keV [8], with most of the calculations [6,7,9,15] giving values closer to the larger values of Ref. [8].

The D^* meson was discovered more than 20 years ago [16] and has been subsequently studied in several experiments at different accelerators e.g. [17–22]. The $D^{*+}(M = 2010.0 \pm 0.5$ MeV) and $D^{*0}(M = 2006.7 \pm 0.5$ MeV) have relatively little phase space for strong decay into $D + \pi$. The current PDG averages [4] for the measured branching ratios of the observed decays are $\text{Br}(D^{*+} \rightarrow D^+\pi^0) : \text{Br}(D^{*+} \rightarrow D^0\pi^+) : \text{Br}(D^{*+} \rightarrow D^+\gamma) = (30.6 \pm 2.5)\% : (68.3 \pm 1.4)\% : (1.1 + 2.1 - 0.7)\%$ and $\text{Br}(D^{*0} \rightarrow D^0\pi^0) : \text{Br}(D^{*0} \rightarrow D^0\gamma) = (61.9 \pm 2.9)\% : (38.1 \pm 2.9)\%$. The most recent experiment on D^{*+} decays [21] gives more accurate branching ratios for the three decay channels as follows: $(30.7 \pm 0.7)\% : (67.6 \pm 0.9)\% : (1.7 \pm 0.6)\%$.

Although there are, by now, good data on the branching ratios, there is still no absolute measurement of any of the partial decay widths. The tightest upper limit has been established by the ACCMOR Collaboration at CERN [22] from the measurement of 127 D^{*+} events using a high-resolution silicon vertex detector, to be $\Gamma(D^{*+}) < 131$ keV. The other closest limit, obtained by the HRS Collaboration [18], gives upper limits of 1.1 MeV and 2.1 MeV for the total decay widths of the charged and neutral D^{*} 's.

The decays of D^* have also been treated extensively in a plethora of theoretical models. Many of the papers we mentioned concerning the B^* decay [5–15] discuss also the D^* decays. In addition, we want to mention the early approaches [23,24] with effective Lagrangian including symmetry breaking, a relativistic quark model [25], the study of D^* decays using the chiral-bag model which contains pion exchange effects (pion loops) [26], the use of QCD sum rules [27], a chiral model with $M_c \rightarrow \infty$ [28] and the comprehensive analy-

sis of Kamal and Xu [29]. Recently [30], the strength of the various decay channels of D^* has been extracted from an analysis of the experimental branching ratios by the use of the chiral perturbation theory.

In the D^* case, the theoretical calculations again span an order of magnitude range for the prediction of the absolute decay widths, from a small width of $\Gamma(D^{*0}) \simeq (3-10)$ keV [14,28] to $\Gamma(D^{*0}) \simeq (60-120)$ keV [9,24,25], including fairly large uncertainties. It should be emphasized at this point that the chiral bag calculation (χ) has offered the best estimation for the branching ratios [26] $\text{Br}^\chi(D^{*+} \rightarrow D^+\pi^0) : \text{Br}^\chi(D^{*+} \rightarrow D^0\pi^+) : \text{Br}^\chi(D^{*+} \rightarrow D^+\gamma) = 31.2\% : 67.5\% : 1.3\%$ and $\text{Br}^\chi(D^{*0} \rightarrow D^0\pi^0) : \text{Br}^\chi(D^{*0} \rightarrow D^0\gamma) = 64.3\% : 35.7\%$.

The recent experiments have confirmed [4,21] these relative ratios and dispersed the puzzling features which prevailed previously concerning the radiative branching ratio and the relative ratios of D^{*+} strong channels (see, e.g., Ref. [29]). The prediction of the chiral bag model [26] is $\Gamma(D^{*+} \rightarrow \text{all}) = 79$ keV, $\Gamma(D^{*0} \rightarrow \text{all}) = 59.4$ keV. Several of the other calculations result in fairly similar values [5,6,29] as well as predicting for $\Gamma(D^{*0})$ a value approximately 25% smaller than for $\Gamma(D^{*+})$. There are also calculations in which these widths are nearly equal [11,14] or, on the contrary, calculations giving $\Gamma(D^{*+})$ to be at least twice larger than $\Gamma(D^{*0})$ [15,27,28].

The experimental and theoretical survey we presented here is obviously of direct relevance to our calculation as the absolute values of B^* and D^* widths will affect the probability of the $B^* \rightarrow B\gamma\gamma$ and $D^* \rightarrow D\gamma\gamma$ future detection.

III. MODEL FOR TWO-PHOTON TRANSITION

Substantial progress has been made in recent years in the treatment of the interactions of heavy mesons containing a single heavy quark with low momentum pions, by the use of an effective Lagrangian [31–33], the so-called ‘‘heavy meson chiral Lagrangian’’ (HM χ L), which embodies two principal symmetries of quantum chromodynamics (for a comprehensive review of this theoretical framework and its applications, see [34]). At the leading order in an $1/M_H$ expansion (M_H is the mass of the heavy meson) and the chiral limit for the light quarks ($m_l \rightarrow 0, l = u, d, s$), the Lagrangian carries flavor and spin symmetry in the heavy meson sector, as well as $SU(3)_L \otimes SU(3)_R$ chiral invariance in the light meson one. We adopt this framework for the calculation of the processes we study here, namely the $B^*(D^*) \rightarrow B(D)\gamma\gamma$ decays, and we shall use it to display the possible usefulness of these transitions for the determination of the $g_{B^*B\pi}, g_{D^*D\pi}$ and $g_{B^*B\gamma}$ couplings.

The heavy vector (B^* or D^*) and pseudoscalar (B or D) mesons are represented by a 4×4 Dirac matrix H , with one spinor index for the heavy quark and the second one for the light degree of freedom:

$$H = \frac{1 + \not{v}}{2} [B_\mu^* \gamma^\mu - B \gamma_5], \quad \bar{H} = \gamma_0 H^\dagger \gamma_0, \quad (3.1)$$

where v is the meson velocity, and $v^\mu B_\mu^* = 0$ and B_μ^*, B are the respective annihilation operators of the meson fields. We

shall usually refer henceforth to $B^* \rightarrow B \gamma \gamma$ with the understanding that the same treatment holds for $D^* \rightarrow D \gamma \gamma$. However, we shall specify the two channels separately when numerical or other specific features make it necessary.

The relevant interaction term of the HM χ L, representing the coupling of heavy mesons to an odd number of pions, is given by [31,32]

$$\mathcal{L}_{\text{HM}\chi\text{L}}^{\text{int}} = g \text{Tr}(\bar{H}_a \gamma_\mu \gamma_5 \mathcal{A}_{ab}^\mu H_b) \quad (3.2)$$

where the axial current \mathcal{A}^μ is

$$\mathcal{A}^\mu = \frac{i}{2} (\xi^\dagger \partial^\mu \xi - \xi \partial^\mu \xi^\dagger) \quad (3.3)$$

and $\xi = \exp(i\mathcal{M}/f)$, with \mathcal{M} being the usual 3×3 matrix describing the octet of pseudoscalar Nambu-Goldstone bosons. The axial coupling constant g is one of the basic parameters of the HM χ L, which is of direct import to our problem. a, b denote light quark flavors ($a, b = 1, 2, 3$) and f is the pion decay constant, $f = 132$ MeV. Expanding the axial current and using the first term $\mathcal{A}^\mu = -(1/f) \partial^\mu \mathcal{M} + \dots$ one obtains the effective Lagrangian representing $B^* B$ -pion and $B^* B^*$ -pion interactions, which are the relevant ones in our problem. Thus,

$$\begin{aligned} \mathcal{L}_{\text{eff}}^1 = & \left[-\frac{2g}{f} B_\mu^* \partial^\mu \mathcal{M} B^\dagger + \text{H.c.} \right] \\ & + \frac{2gi}{f} \epsilon_{\alpha\beta\mu\nu} B^{*\beta} \partial^\mu \mathcal{M} B^{*\dagger\alpha} v^\nu. \end{aligned} \quad (3.4)$$

The dimensionless $B^* B \pi$ coupling is defined as [34]

$$\langle \pi(q) \bar{B}(v_1) | B^*(v_2, \epsilon_2) \rangle = g_{B^* B \pi}(q^2) q_\mu \epsilon_2^\mu \quad (3.5)$$

where ϵ^μ is the polarization vector of B^* , with the physical coupling given by the limit $q^2 \rightarrow m_\pi^2$. We use the same normalization convention as in [34].

Throughout this work, we assume that the variation of $g_{B^* B \pi}$ with q^2 in the region of our treatment can be safely neglected. Likewise, we define

$$\begin{aligned} \langle \pi(q) \bar{B}^*(v_1, \epsilon_1) | B^*(v_2, \epsilon_2) \rangle \\ = g_{B^* B^* \pi}(q^2) \epsilon_{\alpha\beta\mu\nu} \epsilon_1^\alpha \epsilon_2^\beta q^\mu v_1^\nu, \end{aligned} \quad (3.6)$$

with the same remarks as above.

We also note that the isospin symmetry requires

$$\begin{aligned} g_{B^* B \pi} & \equiv g_{B^* + B^0 \pi^+} = -\sqrt{2} g_{B^* + B^+ \pi^0} = \sqrt{2} g_{B^* 0 B^+ \pi^0} \\ & = -g_{B^* 0 B^+ \pi^-} \end{aligned} \quad (3.7)$$

and the $g_{B^* B \pi}$ so defined is the commonly used in the literature.

The relation (3.7) holds similarly for $g_{B^* B^* \pi}, g_{D^* D \pi}$ and $g_{D^* D^* \pi}$ couplings.

Now, from Eqs. (3.2)–(3.4), using the definition (3.5) one has

$$\begin{aligned} g_{B^* B \pi} & = \frac{2M_B}{f} g = g_{B^* B^* \pi} \\ g_{D^* D \pi} & = \frac{2M_D}{f} g = g_{D^* D^* \pi}. \end{aligned} \quad (3.8)$$

Note that, in deriving Eqs. (3.8) one assumes $B, B^*(D, D^*)$ mass degeneracy. In order to calculate the $B^* \rightarrow B \gamma \gamma$ decay width we use the interaction Lagrangian (3.4) to the leading order in chiral perturbation theory, which is an appropriate tool here, in view of the smallness of $M_{B^*} - M_B$.

The calculation of the radiative processes $B^*(D^*) \rightarrow B(D) \gamma \gamma$ obviously requires the incorporation of the electromagnetic interaction in our Lagrangian (3.4), which is performed [30,35] by the usual procedure of gauging the Lagrangian with the $U(1)$ photon field. This leads to the replacement of the derivative operators in the Lagrangian by covariant derivatives containing the photon field, explicitly exhibited in [35]. Nevertheless, the new Lagrangian still does not provide for couplings to induce the observed $B^* \rightarrow B \gamma, D^* \rightarrow D \gamma$ magnetic dipole transitions. This necessitates the introduction of an additional term in the Lagrangian, a contact gauge invariant interaction proportional to the electromagnetic field $F_{\mu\nu}$, which is given by [30,35]

$$\mathcal{L} = \frac{e\mu}{4} \text{Tr}(\bar{H}_a \sigma_{\mu\nu} F_{\mu\nu} H_b \delta_{ab}), \quad (3.9)$$

where μ is the strength of this anomalous magnetic dipole interaction, having mass dimension $[1/M]$.

Additional terms arising from an $1/M_H$ expansion exist [30,35]; however, several of them, including the radiation of the heavy quark, can be absorbed in Eq. (3.9) by redefining μ . In the present paper, we shall consider μ as an effective coupling, representing the strength of the $B^*(D^*) B(D) \gamma$ transition.

Expanding H in terms of the components, one obtains, for the additional electromagnetic interaction,

$$\mathcal{L}_{\text{eff}}^2 = -e\mu F^{\mu\nu} [iB_\mu^{*\dagger} B_\nu^* + \epsilon_{\alpha\beta\mu\nu} v^\alpha (B^\dagger B_\beta^* + \text{H.c.})] \quad (3.10)$$

which exhibits $B^* B \gamma$ and $B^* B^* \gamma$ couplings with equal strength, as given by the heavy quark symmetry. From Eq. (3.10) we obtain the respective vertices, which are

$$\begin{aligned} \langle \gamma(k, \epsilon) \bar{B}^*(v_1, \epsilon_1) | B^*(v_2, \epsilon_2) \rangle \\ = e\mu M_{B^*} (\epsilon_1 \cdot k \epsilon \cdot \epsilon_2 - \epsilon_2 \cdot k \epsilon \cdot \epsilon_1) \end{aligned} \quad (3.11)$$

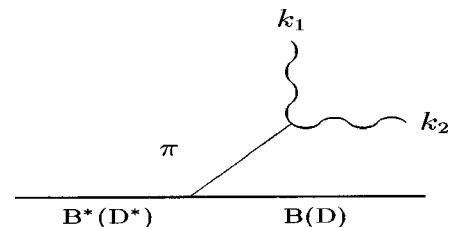


FIG. 1. The anomaly graph for $B^*(D^*) \rightarrow B(D) \gamma \gamma$.

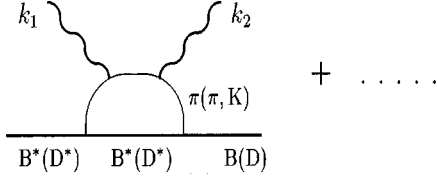


FIG. 2. Loop graph for $B^*(D^*) \rightarrow B(D) \gamma \gamma$ which depends only on the strong coupling. Additional graphs of this kind are discussed in the text.

$$\langle \gamma(k, \epsilon) \bar{B}(v_1) | B^*(v_2, \epsilon_2) \rangle = -ie M_{B^*} \mu \epsilon_{\mu\nu\alpha\beta} \epsilon^\mu k^\nu v_2^\alpha \epsilon_2^\beta. \quad (3.12)$$

The propagator of the heavy vector meson is given by $-i(g^{\mu\nu} - v^\mu v^\nu)/2[(v \cdot k) - \Delta/4]$, where $\Delta = M_{B^*} - M_B$ and v, k are the velocity and the residual momentum. The propagator of the heavy pseudoscalar meson is $i/2[(v \cdot k) + 3\Delta/4]$ [34].

Now, considering Lagrangians (3.4) and (3.10), as well as the axial anomaly responsible for the $\pi^0 \rightarrow \gamma \gamma$, we classify the diagrams contributing to $B^* \rightarrow B \gamma \gamma$ in the leading order of chiral perturbation theory as follows:

There is the diagram $B^{*0} \rightarrow B^{*+} \pi^- \rightarrow B^0 \gamma \gamma$ (Fig. 1), via a virtual pion (the somewhat different situation in $D^* \rightarrow D \gamma \gamma$ will be analyzed in the last section). This diagram contains the known strength of the pion axial anomaly. Then, there is the loop graph $B^{*0} \rightarrow (B^{*+} \pi^-) \rightarrow B^0 \gamma \gamma$ (Fig. 2), with the photons radiated from the virtual charged pion in the loop, with additional graphs of the same class, as specified in the next section. The first graph is proportional to the $g_{B^* B \pi}$ coupling, while the loop graph contains the $g_{B^* B \pi} g_{B^* B^* \pi}$ product. In addition we have the tree level diagram with two insertions of the magnetic operator defined in Eq. (3.10), leading to $B^{*0} \rightarrow B^{*0} \gamma \rightarrow B^0 \gamma \gamma$ (Fig. 3). This graph depends only on the μ magnetic moment. Finally we have a class of one loop diagrams which involve both the magnetic moment and the strong coupling, which is exhibited in Figs. 4–6. We did not include the contribution of diagrams containing three heavy meson propagators which is negligible. Needless to say, the determination of $g_{B^* B \pi}$ would be simpler, should the first two graphs dominate. However, this is not true for D^* decay, while it can be true for the B^* decay for an opportune range of parameters as we discuss in the next section.

We remark at this point that corrections to Eq. (3.2) which arise from higher terms in the $1/M_H$ expansion as well as in chiral breaking have also been investigated [30,34,36,37]. A comprehensive inclusion of these corrections in the calculation of the two-photon decays of heavy vector mesons is beyond our scope in this first treatment of these processes.

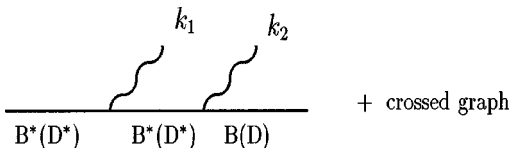


FIG. 3. Tree graph for $B^*(D^*) \rightarrow B(D) \gamma \gamma$.

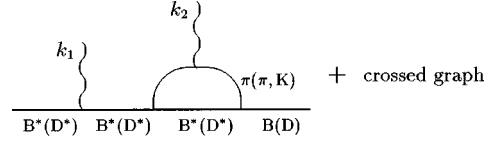


FIG. 4. Loop graph for $B^*(D^*) \rightarrow B(D) \gamma \gamma$ which involve both magnetic and the strong couplings. Instead of $B^*(D^*)$ in the first propagator we can have $B(D)$.

Nevertheless, we note that we shall use physical masses for the degenerate doublet of heavy mesons both in the loop propagators and in the decay calculations; moreover, the chiral loops included are themselves of order $1/M_H$. The terms we include are the leading ones in chiral perturbation theory, and are of the same order in an $1/N_c$ expansion; moreover, to this order there are no counterterms [38].

It is appropriate to mention now that the $g_{B^* B \pi}, g_{D^* D \pi}$ couplings were estimated in recent years by the use of a variety of theoretical techniques, such as QCD sum rules [14,27], soft pion approximation [39] and other methods [9,10,30,36,37,40]. Generally, the values of g obtained in these works are in the range $g=0.25-0.7$, significantly smaller than the quark model result of $g=1$ or of modified quark models [24,41,42] which brought this value slightly below 1. The most recent determinations of g include an analysis [34] of various theoretical approaches which leads to a ‘‘best estimate’’ of $g=0.38$, a recent lattice determination giving $0.42(4)(8)$ [43] and the analysis of Stewart [30] which incorporates symmetry breaking terms in the Lagrangian and obtains $g=0.27^{+0.09}_{-0.04}$.

Finally, the experimental limit $\Gamma(D^{*+}) < 131$ keV [22] puts an upper limit of $g < 0.71$, using $\Gamma(D^{*+} \rightarrow D^0 \pi^+ + D^+ \pi^0) = (g^2/4\pi f^2) |\vec{p}_\pi|^3$.

The existing theoretical estimates we mentioned, give $0.04 \text{ keV} < \Gamma(B^{*0} \rightarrow B^0 \gamma) < 1 \text{ keV}$ and $0.10 \text{ keV} < \Gamma(B^{*+} \rightarrow B^+ \gamma) < 1 \text{ keV}$, where we allowed for a slightly higher upper limit. We redefine the magnetic coupling in Eq. (3.10) to a dimensionless quantity $\bar{\mu} = M_{B^*} \mu = g_{B^* 0 B^0 \gamma}$ and $\bar{\mu}_+ = M_{B^*} \mu_+ = g_{B^* + B^+ \gamma}$; then the above limits give the ranges $2.2 < \bar{\mu} < 11.0$ and $3.5 < \bar{\mu}_+ < 11.0$.

IV. THE DECAY AMPLITUDES

We present now the explicit expressions of the decay amplitudes, which in our approach, to leading order in chiral perturbation theory, consist of the contribution of the anomaly graph (Fig. 1), the tree level graph (Fig. 3) and the loop graphs (Figs. 2, 4–6).

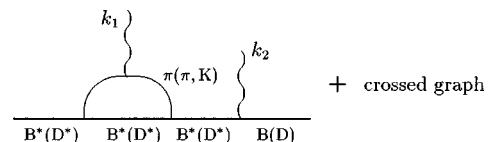


FIG. 5. Loop graph for $B^*(D^*) \rightarrow B(D) \gamma \gamma$ which involve both magnetic and the strong couplings. Instead of $B^*(D^*)$ in the loop we can have $B(D)$.

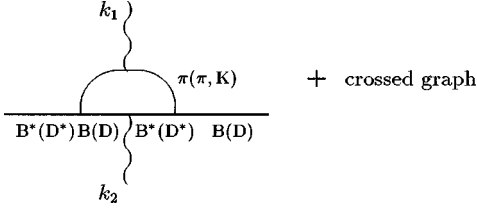


FIG. 6. Loop graph for $B^*(D^*) \rightarrow B(D) \gamma \gamma$ which involve both magnetic and the strong couplings.

In presenting the differential decay distribution, we use the following variables:

$$\begin{aligned} s &= (p - p')^2 = (k_1 + k_2)^2 \\ t &= (p - k_1)^2 = (p' + k_2)^2 \\ u &= (p - k_2)^2 = (p' + k_1)^2 \end{aligned} \quad (4.1)$$

with

$$t + s + u = M_{B^*}^2 + M_B^2, \quad (4.2)$$

where k_1, k_2 are the four-momenta of the two photons and p, p' are the four-momenta of the decaying B^* and the final B respectively. The allowed ranges for s and t are

$$\begin{aligned} 0 \leq s \leq (M_{B^*} - M_B)^2, \quad t_- \leq t \leq t_+, \\ t_{\pm} = \frac{1}{2} [(M_{B^*}^2 + M_B^2 - s) \\ \pm \sqrt{(M_{B^*}^2 + M_B^2 - s)^2 - 4M_{B^*}^2 M_B^2}]. \end{aligned} \quad (4.3)$$

The amplitudes are given for $B^{*0} \rightarrow B^0 \gamma \gamma$ and we shall remark on the changes appearing in $D^{*0} \rightarrow D^0 \gamma \gamma$ whenever required. The amplitude from the anomaly graph, mediated by a pion, is

$$\begin{aligned} A_{\text{anomaly}}(B^{*0} \rightarrow B^0 \gamma \gamma) &= \frac{\alpha g_{B^* B \pi} g_{B^* B^* \pi}}{\sqrt{2} \pi f} \epsilon_{B^*}^{\mu} \epsilon_1^{\lambda} \epsilon_2^{\gamma} \frac{1}{s - m_{\pi}^2} \\ &\times \epsilon_{\lambda \gamma \tau \rho} k_1^{\tau} k_2^{\rho} (k_1 + k_2)_{\mu}, \end{aligned} \quad (4.4)$$

where $\epsilon_{B^*}, \epsilon_1, \epsilon_2$ are the polarization vectors of the heavy vector meson B^* and the two photons respectively. There are additional contributions from η, η' which are not specified in Eq. (4.4). As we shall describe in the next section, their contribution is rather small and we may safely neglect them at this stage.

For the tree level graph we find

$$\begin{aligned} A_{\text{tree}}(B^{*0} \rightarrow B^0 \gamma \gamma) &= \frac{4 \pi \alpha \bar{\mu}^2}{M_{B^*}} \epsilon_{\gamma \delta \alpha \beta} \epsilon_{B^* \sigma} p'^{\alpha} \\ &\times \left[\frac{\epsilon_2^{\gamma} k_2^{\delta} (\epsilon_1^{\sigma} k_1^{\beta} - \epsilon_1^{\beta} k_1^{\sigma})}{t - M_{B^*}^2} + \frac{\epsilon_1^{\gamma} k_1^{\delta} (\epsilon_2^{\sigma} k_2^{\beta} - \epsilon_2^{\beta} k_2^{\sigma})}{u - M_{B^*}^2} \right] \end{aligned} \quad (4.5)$$

The loop contribution which depends only on the strong coupling is given by a sum of several diagrams. In addition to that explicitly shown in Fig. 2 there are diagrams with one photon radiated by the virtual pion in the loop and the other emitted from the $B^* B^* \pi$, $B^* B \pi$ vertices or both photons emitted from these vertices, or both photons emitted from the loop by the $\pi \pi \gamma \gamma$ vertex. In the limit of photon momenta small compared to the pion mass, which we find to be a suitable approximation, the class of diagrams of Fig. 2 gives

$$\begin{aligned} A_{\text{loop}}^1(B^{*0} \rightarrow B^0 \gamma \gamma) &= \frac{\alpha g_{B^* B \pi} g_{B^* B^* \pi}}{8 \pi M_{B^*}} \epsilon_{\mu \eta \alpha \beta} \epsilon_{B^*}^{\mu} v^{\beta} \epsilon_1^{\lambda} \epsilon_2^{\gamma} (k_1 + k_2)^{\eta} \\ &\times \left[3(g_{\gamma}^{\alpha} v_{\lambda} + g_{\lambda}^{\alpha} v_{\gamma}) + \frac{1}{9 m_{\pi}} (g_{\gamma}^{\alpha} k_{2\lambda} + g_{\lambda}^{\alpha} k_{1\gamma}) \right]. \end{aligned} \quad (4.6)$$

Finally other loop contributions to the $B^* \rightarrow B \gamma \gamma$ decay come from diagrams where both the strong coupling and the magnetic one are involved. There are diagrams with one photon radiated by the virtual pion in the loop and the other emitted from the ingoing B^* particle through the $B^* B^* (B) \gamma$ vertices (Fig. 4), or from the outgoing particle B^* which becomes B through the $B^* B \gamma$ vertex (Fig. 5), or from the B in the loop which becomes B^* through the $B^* B \gamma$ vertex (Fig. 6).

The amplitude corresponding to Fig. 4 with a $B^* B^* \gamma$ vertex is

$$\begin{aligned} A_{\text{loop}}^2(B^{*0} \rightarrow B^0 \gamma \gamma) &= \frac{11 \alpha (M_{B^*} - M_B) g_{B^* B^* \pi} g_{B^* B \pi} \bar{\mu}}{16 \pi M_{B^*}^2} \epsilon_{\alpha \sigma \gamma \delta} \\ &\times \left[[k_1^{\alpha} (\epsilon_{B^*} \cdot \epsilon_1) - \epsilon_1^{\alpha} (\epsilon_{B^*} \cdot k_1)] \frac{(p - k_1)^{\delta} \epsilon_2^{\gamma} k_2^{\sigma}}{t - M_{B^*}^2} \right. \\ &\left. + [k_2^{\alpha} (\epsilon_{B^*} \cdot \epsilon_2) - \epsilon_2^{\alpha} (\epsilon_{B^*} \cdot k_2)] \frac{(p - k_2)^{\delta} \epsilon_1^{\gamma} k_1^{\sigma}}{u - M_{B^*}^2} \right]. \end{aligned} \quad (4.7)$$

The amplitude corresponding to Fig. 4, where a $B^* B \gamma$ vertex replaces the $B^* B^* \gamma$ appearing in Fig. 4, is

$$\begin{aligned} A_{\text{loop}}^3(B^{*0} \rightarrow B^0 \gamma \gamma) &= \frac{9 \alpha m_{\pi}^2 g_{B^* B \pi}^2 \bar{\mu}}{4 \pi M_{B^*}} \epsilon_{\mu \nu \alpha \beta} \epsilon_{B^*}^{\nu} v^{\alpha} v_{\gamma} \\ &\times \left[\frac{\epsilon_1^{\mu} k_1^{\beta} \epsilon_2^{\gamma}}{t - M_{B^*}^2} + \frac{\epsilon_2^{\mu} k_2^{\beta} \epsilon_1^{\gamma}}{u - M_{B^*}^2} \right]. \end{aligned} \quad (4.8)$$

The amplitude corresponding to Fig. 5 with B in the loop is

$$\begin{aligned}
A_{\text{loop}}^4(B^{*0} \rightarrow B^0 \gamma \gamma) &= \frac{3\alpha m_\pi^2 g_{B^*B\pi}^2 \bar{\mu}}{8\pi M_{B^*}^2} \epsilon_{\mu\nu\alpha\rho} \epsilon_{B^*}^\sigma (g_\gamma^\rho v_\sigma + g_\sigma^\rho v_\gamma) \\
&\times \left[\frac{(p-k_1)^\alpha \epsilon_2^\mu k_2^\nu \epsilon_1^\gamma}{t-M_{B^*}^2} + \frac{(p-k_2)^\alpha \epsilon_1^\mu k_1^\nu \epsilon_2^\gamma}{u-M_{B^*}^2} \right]
\end{aligned} \tag{4.9}$$

and the one with B^* in the loop is

$$\begin{aligned}
A_{\text{loop}}^5(B^{*0} \rightarrow B^0 \gamma \gamma) &= \frac{3\alpha m_\pi^2 g_{B^*B^*\pi}^2 \bar{\mu}}{16\pi M_{B^*}^3} \\
&\times \epsilon_{\alpha\beta\gamma\delta} \epsilon_{B^*}^\beta v^\delta \epsilon_{\eta\alpha\xi\rho} \epsilon_{\mu\nu\sigma\eta} (g^{\gamma\rho} v_\tau + g_\tau^\gamma v^\rho) \\
&\times \left[\frac{(p-k_1)^\xi (p-k_1)^\sigma \epsilon_1^\tau \epsilon_2^\mu k_2^\nu}{t-M_{B^*}^2} \right. \\
&\left. + \frac{(p-k_2)^\xi (p-k_2)^\sigma \epsilon_1^\mu \epsilon_2^\tau k_1^\nu}{u-M_{B^*}^2} \right].
\end{aligned} \tag{4.10}$$

Finally the amplitude corresponding to Fig. 6 is

$$\begin{aligned}
A_{\text{loop}}^6(B^{*0} \rightarrow B^0 \gamma \gamma) &= \frac{11\alpha g_{B^*B\pi}^2 \bar{\mu}_+}{24\pi M_{B^*}^3} \epsilon_{\mu\nu\alpha\beta} \epsilon_{B^*}^\sigma \\
&\times \left[\frac{1}{3} (k_1+k_2)_\sigma \epsilon_1^\alpha \epsilon_2^\mu k_1^\nu k_2^\beta + \frac{1}{2} p^\alpha \right. \\
&\left. \times [\epsilon_2^\mu k_2^\beta (\epsilon_{1\sigma} k_1^\nu + \epsilon_{1\nu} k_1^\sigma) + \epsilon_1^\mu k_1^\beta (\epsilon_{2\sigma} k_2^\nu + \epsilon_{2\nu} k_2^\sigma)] \right].
\end{aligned} \tag{4.11}$$

In the B^* decay, the pions are the sole contributions in the loop, while in the $D^* \rightarrow D \gamma \gamma$ calculation we include both pions and kaons.

Let us call A the sum of all the amplitudes:

$$A = A_{\text{anomaly}} + A_{\text{tree}} + A_{\text{loops}} \tag{4.12}$$

where A_{loops} is the sum of all the amplitudes $A_{\text{loops}}^i, i = 1, \dots, 6$, which come from the loops.

The square of the above amplitude, when averaged over the initial spin and summed over the final spins, is

$$|\bar{A}|^2 = \frac{1}{2} \sum_{\text{spins}} |A|^2, \tag{4.13}$$

where we have included the factor $\frac{1}{2}$ in order to take into account two identical particles in the final state.

The differential decay rate of photon energy is obtained by integrating the following expression over the variable t :

$$\frac{d\Gamma}{ds} = \frac{1}{(2\pi)^3} \frac{1}{32M_{B^*}^3} \int_{t_-}^{t_+} |\bar{A}|^2 dt. \tag{4.14}$$

There is a major difference in the anomaly contribution of the B^* and D^* decays. Since the π^0 appears in the physical region in the $D^{*0} \rightarrow D^0 \pi^0$ decay, we have to isolate the on-shell π^0 decay in the $D^{*0} \rightarrow D^0 \gamma \gamma$ mode. Hence, for the D^* case we limit ourselves in the integration of $d\Gamma/ds$ to a region which goes from $s=0$ up to 20 MeV away from the pion mass.

Using now the physical masses of $M_{B^*}, M_B, M_{D^*}, M_D$ [4] and Eq. (3.8) we obtain, for the decay rates of $B^* \rightarrow B \gamma \gamma$, the following expression:

$$\begin{aligned}
\Gamma(B^* \rightarrow B \gamma \gamma) &= (3.40 \times 10^{-16} g^2 + 1.53 \times 10^{-12} g^4 + 4.81 \times 10^{-17} g^3 \bar{\mu} + 1.53 \times 10^{-13} g^4 \bar{\mu} + 4.71 \times 10^{-17} g \bar{\mu}^2 \\
&+ 9.81 \times 10^{-14} g^4 \bar{\mu}^2 + 2.65 \times 10^{-16} g^2 \bar{\mu}^3 + 1.38 \times 10^{-16} \bar{\mu}^4 + 2.67 \times 10^{-16} g^3 \bar{\mu}_+ + 2.90 \times 10^{-17} g^4 \bar{\mu}_+ \\
&+ 8.94 \times 10^{-20} g^4 \bar{\mu} \bar{\mu}_+ + 9.11 \times 10^{-20} g^2 \bar{\mu}^2 \bar{\mu}_+ + 7.21 \times 10^{-17} g^4 \bar{\mu}_+^2) \text{ GeV}.
\end{aligned} \tag{4.15}$$

As we can see this is a function of both the strong coupling g and the magnetic dipole strength $\bar{\mu}, \bar{\mu}_+$ which represent the effective $g_{B^*0B^0\gamma}$ and $g_{B^*+B^+\gamma}$ couplings. For the $D^* \rightarrow D \gamma \gamma$ we have

$$\begin{aligned}
\Gamma(D^* \rightarrow D \gamma \gamma) &= (2.52 \times 10^{-11} g^2 + 5.85 \times 10^{-10} g^4 + 1.79 \times 10^{-12} g^3 \bar{\mu} + 4.43 \times 10^{-11} g^4 \bar{\mu} + 1.30 \times 10^{-12} g \bar{\mu}^2 \\
&+ 3.50 \times 10^{-11} g^4 \bar{\mu}^2 + 2.42 \times 10^{-13} g^2 \bar{\mu}^3 + 2.18 \times 10^{-12} \bar{\mu}^4 + 1.01 \times 10^{-11} g^3 \bar{\mu}_+ + 2.95 \times 10^{-13} g^4 \bar{\mu}_+ \\
&+ 2.11 \times 10^{-14} g^4 \bar{\mu} \bar{\mu}_+ + 1.70 \times 10^{-14} g^2 \bar{\mu}^2 \bar{\mu}_+ + 2.05 \times 10^{-12} g^4 \bar{\mu}_+^2) \text{ GeV}.
\end{aligned} \tag{4.16}$$

In this case we can relate the magnetic coupling to the strong coupling using the existing experimental informations on $\Gamma(D^{*0} \rightarrow D^0 \pi^0) : \Gamma(D^{*0} \rightarrow D^0 \gamma)$ of $(61.9 \pm 2.9)\% : (38.1 \pm 2.9)\%$, which gives rise to the relation $\bar{\mu} \approx 6.6g$, and $\Gamma(D^{*+} \rightarrow D^0 \pi^+) : \Gamma(D^{*+} \rightarrow D^+ \gamma)$ of $(67.6 \pm 0.9)\% : (1.7 \pm 0.6)\%$, which gives rise to the relation $\bar{\mu}_+ \approx 1.7g$. Then we can write the decay width solely as a function of g , which is a crucial step in the engagement of this decay as a tool for measuring g :

$$\begin{aligned} \Gamma(D^* \rightarrow D \gamma \gamma) = & (2.52 \times 10^{-11} g^2 + 5.66 \times 10^{-11} g^3 + 4.76 \\ & \times 10^{-9} g^4 + 3.64 \times 10^{-10} g^5 \\ & + 1.53 \times 10^{-9} g^6) \text{ GeV}. \end{aligned} \quad (4.17)$$

We used in Eqs. (4.15), (4.16) the same notation of μ, μ_+ for the magnetic moment strength in both the charmed and b -flavored sectors although they are probably not equal for the physical processes. However, since in the charm case the magnetic coupling has been related to the strong one, the μ, μ_+ will denote in the rest of the paper the strength of the $B^{*0,+} \rightarrow B^{0,+} \gamma$ transitions.

The experimentally measured branching ratios of $D^* \rightarrow D \pi$, $D^* \rightarrow D \gamma$ lead to relations between $\bar{\mu}, \bar{\mu}_+$ and g modulo an unknown phase. We have allowed also for the possibilities of negative relative signs among $\bar{\mu}, \bar{\mu}_+$ and g and as it turns out, this affects only slightly the numerical picture, due to the fact that the main contribution is given by quadratic terms. In Eq. (4.18) we give for comparison the expression obtained for $\bar{\mu} = -6.6g, \bar{\mu}_+ = -1.7g$:

$$\begin{aligned} \Gamma(D^* \rightarrow D \gamma \gamma)_{\bar{\mu}=\text{neg}} = & (2.52 \times 10^{-11} g^2 \\ & + 5.66 \times 10^{-11} g^3 + 4.70 \times 10^{-9} g^4 \\ & - 3.64 \times 10^{-10} g^5 + 1.53 \\ & \times 10^{-9} g^6) \text{ GeV}. \end{aligned} \quad (4.18)$$

This ambiguity will be further discussed in the next section. The difference between the rates of B^* and D^* is mainly due to the different phase space.

In discussing the two photon radiative decays, we shall refer in the next section to the following quantities:

$$\text{Br}(B^* \rightarrow B \gamma \gamma) = \frac{\Gamma(B^{*0} \rightarrow B^0 \gamma \gamma)}{\Gamma(B^{*0})} = \frac{\Gamma(B^{*0} \rightarrow B^0 \gamma \gamma)}{\Gamma(B^{*0} \rightarrow B^0 \gamma)} \quad (4.19)$$

$$\begin{aligned} \text{Br}(D^* \rightarrow D \gamma \gamma) = & \frac{\Gamma(D^{*0} \rightarrow D^0 \gamma \gamma)}{\Gamma(D^{*0})} \\ = & \frac{\Gamma(D^{*0} \rightarrow D^0 \gamma \gamma)}{\Gamma(D^{*0} \rightarrow D^0 \gamma) + \Gamma(D^{*0} \rightarrow D^0 \pi^0)}. \end{aligned} \quad (4.20)$$

V. DISCUSSION AND CONCLUSIONS

The formalism we have presented refers to the decays of the neutral heavy vector mesons B^{*0}, D^{*0} , as it will the nu-

merical analysis of our results, which will be given below. For the charged decays, $B^{*+} \rightarrow B^+ \gamma \gamma$ and $D^{*+} \rightarrow D^+ \gamma \gamma$, one has to consider also the bremsstrahlung emission which appears in diagrams of Figs. 3 and 4 and additional ones. The bremsstrahlung radiation comes from the initial or the final charged particles. To give an idea of this effect we have calculated the part of the bremsstrahlung amplitude which is due to radiation from the final B^+ particle in the amplitude $B^{*+} \rightarrow (B^+ \gamma) \rightarrow B^+ \gamma \gamma$. It is

$$A_{\text{brem}}^{B^+} = 4 \pi \alpha g_{B^* B \gamma} \epsilon_{B^*}^\mu \epsilon_1^\lambda \epsilon_2^\gamma p^\alpha \left[\frac{\epsilon_{\lambda \mu \alpha \beta} k_1^\beta p_\gamma'}{(t - M_B^2)} + \frac{\epsilon_{\gamma \mu \alpha \rho} k_2^\rho p_\lambda'}{(u - M_B^2)} \right]. \quad (5.1)$$

This amplitude (and the ones given by B^{*+} radiation) has to be added in order to get the full amplitude for the $B^{*+} \rightarrow B^+ \gamma \gamma$ decay. An estimate of the bremsstrahlung decay width, from Eq. (5.1) only, using for the unknown $g_{B^* B \gamma}$ vertex a value leading to $\Gamma(B^{*+} \rightarrow B^+ \gamma) = 0.14 \text{ keV}$ [34] leads to a decay width of $\sim 10^{-9} \text{ GeV}$ for $k_1, k_2 \geq 10 \text{ MeV}$, considerably larger than Eq. (4.15). The use of the charged $B^{*+} \rightarrow B^+ \gamma \gamma$ thus involves a different type of analysis in view of the relative size of the different components of $|A(B^{*+} \rightarrow B^+ \gamma \gamma)|^2$ and is less useful for a determination of g . A similar situation is encountered for $D^{*+} \rightarrow D^+ \gamma \gamma$. Thus, we concentrate here on the ‘‘safer’’ neutral decays and we relegate the discussion of the charged decays to a separate work, in which we consider the usefulness of $\Gamma(B^{*+} \rightarrow B^+ \gamma \gamma)$ for the determination of $g_{B^* B \gamma}$ [44].

We proceed now to analyze the results on the two decays separately and we start with $D^{*0} \rightarrow D^0 \gamma \gamma$ transition for which the rate (4.17) was obtained.

The many theoretical estimates for g we mentioned in Sec. III are spread over the range $0.25 < g < 1$ [we also remind the reader that the experimental result [22] on the upper limit of $\Gamma(D^{*+} \rightarrow \text{all})$ can be interpreted as $g < 0.71$]. Using this range and Eqs. (4.17), (4.18), we can establish the expectation

$$\Gamma(D^{*0} \rightarrow D^0 \gamma \gamma) \approx (0.022 - 6.73) \text{ eV}. \quad (5.2)$$

The most promising feature of the present analysis arises when we use the existing experimental informations on $\Gamma(D^{*0} \rightarrow D^0 \pi^0) : \Gamma(D^{*0} \rightarrow D^0 \gamma)$ of $(61.9 \pm 2.9)\% : (38.1$

TABLE I. Predictions for the various $D^* \rightarrow D \gamma \gamma$ decay for various values of g [Eq. (5.5)].

g	$\text{Br}(D^*)$	$\text{Br}(D^*)$
	$(\bar{\mu} = 6.6g, \bar{\mu}_+ = 1.7g)$	$(\bar{\mu} = -6.6g, \bar{\mu}_+ = -1.7g)$
$g = 0.25$	1.7×10^{-6}	1.7×10^{-6}
$g = 0.38$	3.9×10^{-6}	3.7×10^{-6}
$g = 0.5$	6.9×10^{-6}	6.3×10^{-6}
$g = 0.7$	1.4×10^{-5}	1.3×10^{-5}
$g = 1$	3.3×10^{-5}	2.9×10^{-5}

$\pm 2.9\%$ to transform Eq. (4.20) into a ratio of $\Gamma(D^{*0} \rightarrow D^0 \gamma \gamma)$ to the total D^{*0} width which becomes proportional to g^2 .

Using

$$\Gamma(D^{*0} \rightarrow D^0 \pi^0) = \frac{1}{12\pi} \frac{g^2}{f^2} |\vec{p}_\pi|^3 = 1.25 \times 10^{-4} g^2 \text{ GeV} \quad (5.3)$$

and the $(61.9 \pm 2.9)\% : (38.1 \pm 2.9)\%$ relative branching ratio, we arrive at

$$\Gamma(D^{*0} \rightarrow \text{all}) = (2.02 \pm 0.12) \times 10^{-4} g^2 \text{ GeV}. \quad (5.4)$$

Thus from Eqs. (5.4) with (4.17) we can obtain a branching ratio which depends on g^2 only:

$$\text{Br}(D^{*0} \rightarrow D^0 \gamma \gamma) = \frac{(0.025 + 0.057g + 4.76g^2 + 0.36g^3 + 1.53g^4) \times 10^{-9} g^2}{2.02 \times 10^{-4} g^2}. \quad (5.5)$$

With our model for $D^{*0} \rightarrow D^0 \gamma \gamma$, the measurement of this ratio will thus constitute a measurement of the g coupling. Using again the accepted expectation of $0.25 \leq g \leq 1$, we predict

$$\text{Br}(D^* \rightarrow D \gamma \gamma) = \frac{\Gamma(D^{*0} \rightarrow D^0 \gamma \gamma)}{\Gamma(D^*)} = (0.16 - 3.3) \times 10^{-5}. \quad (5.6)$$

A few remarks are in order: first, the sign question. The observed branching ratios do not afford to establish experimentally the sign of $g/g_{D^{*0}D^0\gamma}$. On the other hand, there is theoretical support from the analysis of Stewart [30] on the positive sign of this ratio. However, even if we assume opposite sign for various pairs of the couplings, we found that the changes are rather small, and this is explicitly exhibited in Table I, and included in Eq.(5.6).

The differential distribution in the s variable can also be used to learn about the value of g , due to the fact that the different contributions depend on different powers of g . Finally we remark that the contributions from the diagrams exhibited in Fig. 4 are rather small, as a result of two heavy propagators. The main contributions are those of the

anomaly and of the graphs of Figs. 2 and 3. In Figs. 7 and 8 we present the differential distributions in s for $g=0.7$ and $g=0.25$. In the latter, the contributions containing a higher power of g are diminished and the effect of the anomaly becomes visible in the higher end of the spectrum.

Turning now to the $B^* \rightarrow B \gamma \gamma$, we have a rather different situation. First, there is only one major decay of B^* , namely $B^* \rightarrow B \gamma$, which precludes an analysis like in D^* decays. The branching ratio (4.19) depends on three parameters, $g_{B^*B\pi}$ (or g), $g_{B^*B^0\gamma}$ (or μ) and $g_{B^*B^+\gamma}$ (or μ^+). At this point, we rely on the theoretical estimates presented in Sec. II and constrain our analysis to the regions given by existing calculations.

Now, an inspection of Eq. (4.16) shows that μ_+ , which appears only in diagram of Fig. 6, has a very little effect on the rate, whether μ, μ_+ are at the lowest or at the highest end of their value, for any value of g . Hence, we continue our analysis in the parameter space of $[g, \mu]$ only.

In Table II we present the values of $\text{Br}(B^* \rightarrow B \gamma \gamma)$ for different values of g and the two extreme values of μ , corresponding to $\Gamma(B^* \rightarrow B \gamma) = 40 \text{ eV}$ and 1 keV . Again, assuming that relative negative signs are possible we give in the last column the branching ratio for $\mu = -2.2$. Clearly, a

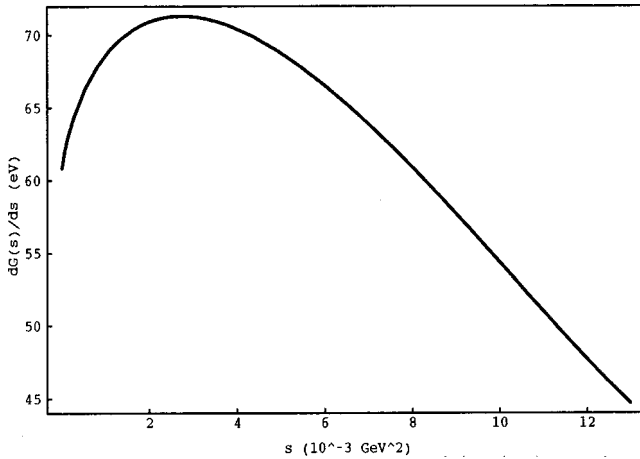


FIG. 7. The differential decay width $d\Gamma(D^* \rightarrow D \gamma \gamma)/ds$ (eV) as a function of s with the value $g=0.7$.

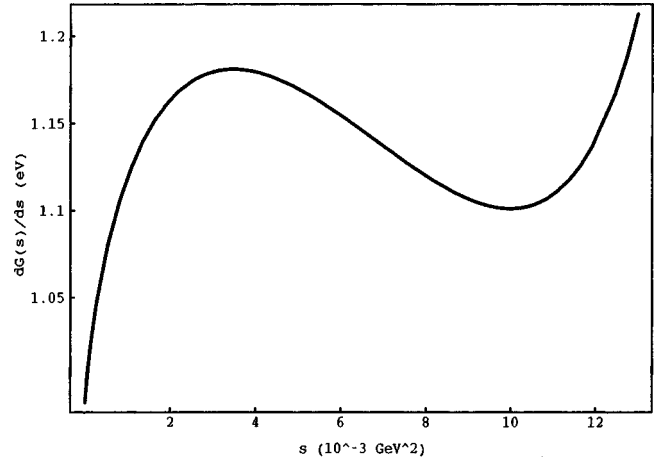


FIG. 8. The differential decay width $d\Gamma(D^* \rightarrow D \gamma \gamma)/ds$ (eV) as a function of s with the value $g=0.25$.

TABLE II. Predictions for the various $B^* \rightarrow B \gamma \gamma$ decay different values of g and μ .

g	$\text{Br}(B^*)(\bar{\mu}=2.2)$	$\text{Br}(B^*)(\bar{\mu}=11.0)$	$\text{Br}(B^*)(\bar{\mu}=-2.2)$
$g=0.25$	3.1×10^{-7}	1.9×10^{-6}	2.4×10^{-7}
$g=0.38$	1.3×10^{-6}	2.2×10^{-6}	9.4×10^{-7}
$g=0.5$	3.7×10^{-6}	2.9×10^{-6}	2.7×10^{-6}
$g=0.7$	1.4×10^{-5}	5.5×10^{-6}	9.2×10^{-6}
$g=1$	4.8×10^{-5}	9.0×10^{-6}	3.8×10^{-5}

branching ratio in the 10^{-7} – 10^{-6} range will not allow one to pinpoint accurate values for the two couplings.

Nevertheless, if the branching ratio turns out to be in the 10^{-5} range, it can only be caused by large values of g , say $g > 0.6$.

We wish also to mention an additional scenario: the g coupling will probably be measured directly in D^* decays, or indirectly from $\text{Br}(D^{*0} \rightarrow D^0 \gamma \gamma)$ or other methods. With this knowledge, $\text{Br}(B^{*0} \rightarrow B^0 \gamma \gamma)$ becomes a function of $g_{B^*0 B^0 \gamma}$ only and it could provide the desirable measurement of this coupling. This is a very interesting issue, since as pointed out already some time ago [26], there is no other possibility of measuring the width of the $B^* \rightarrow B \gamma$ decay with presently known techniques.

In Figs. 9, 10, and 11 we give the differential distribution of $d\Gamma(B^* \rightarrow B \gamma \gamma)/ds$ for $g=0.5$ and three different values of μ . Clearly, once g is known one may use accurate differential distributions to distinguish between different μ values.

At this point we also wish to make some remarks on the similar decays of the strange heavy vector mesons, $B_s^{*0} \rightarrow B_s^0 \gamma \gamma$ and $D_s^{*+} \rightarrow D_s^+ \gamma \gamma$, which were not mentioned so far. In both these cases the pion anomaly is further suppressed, since $B_s^{*0} \rightarrow B_s^0 \pi^0$, $D_s^{*+} \rightarrow D_s^+ \pi^0$ can proceed only by isospin violation, e.g., via η – π^0 mixing. On the other hand, both decays can proceed via chiral loops with charged K mesons in the loops, $B_s^{*0} \rightarrow (K^+ B^{*-}) \rightarrow B_s^0 \gamma \gamma$ and $D_s^{*+} \rightarrow (K^+ D^{*0}) \rightarrow D_s^+ \gamma \gamma$. However, one must add that for $D_s^{*+} \rightarrow D_s^+ \gamma \gamma$ there is the complication of the bremsstrahlung and we shall disregard it here.

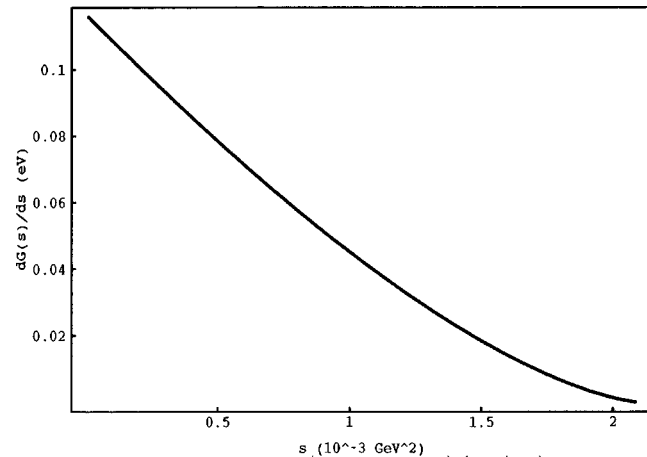


FIG. 9. The differential decay width $d\Gamma(B^* \rightarrow B \gamma \gamma)/ds$ (eV) as a function of s with the value $g=0.5$ and $\mu=2.2$.

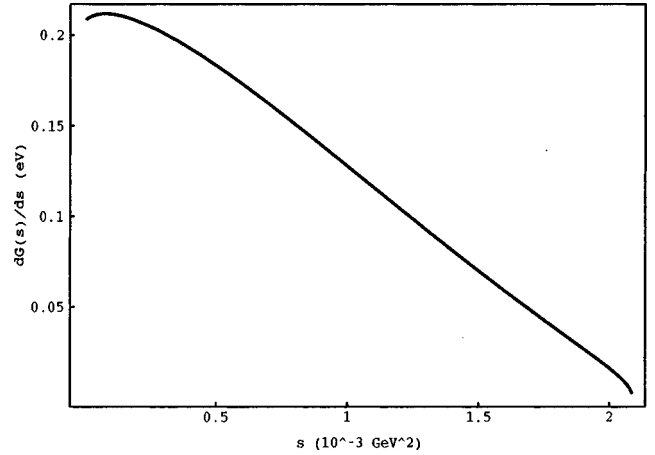


FIG. 10. The differential decay widths $d\Gamma(B^* \rightarrow B \gamma \gamma)/ds$ (eV) as a function of s , with the value $g=0.5$ and $\mu=5.7$.

We calculated therefore only the $B_s^{*0} \rightarrow B_s^0 \gamma \gamma$ decay, and the situation is quite similar to that encountered in B^{*0} decay; therefore we do not repeat this analysis here.

Before concluding we comment on a few points which were neglected in our treatment.

(1) We calculated also the contribution to the anomaly term of a virtual η exchange for the $D^* \rightarrow D \gamma \gamma$ decay. The inclusion of η modifies our result in Eq. (4.16) by a factor of $(1 + g_{D^* D \eta}/10g_{D^* D \pi})$. Since $g_{D^* D \eta}$ and $g_{D^* D \pi}$ are expected to be comparable, this is a small effect.

(2) We neglected the off-shell q^2 dependence of the anomaly which could have some effect, especially in the D^* decay. This should be included in a more detailed treatment.

To summarize, we have used the heavy meson chiral Lagrangian to present the first treatment of the rare $B^{*0} \rightarrow B^0 \gamma \gamma$, $D^{*0} \rightarrow D^0 \gamma \gamma$. The decay rates depend on the strong $g_{B^* B \pi}$, $g_{D^* D \pi}$ couplings and on the strength of the magnetic dipole transitions $g_{B^* B \gamma}$, $g_{D^* D \gamma}$. The strong couplings are expressed in the chiral Lagrangian by the strong axial coupling g .

We have shown that $\text{Br}(D^{*0} \rightarrow D^0 \gamma \gamma)$ can be given as a function of g only, and as such, it would provide an appro-

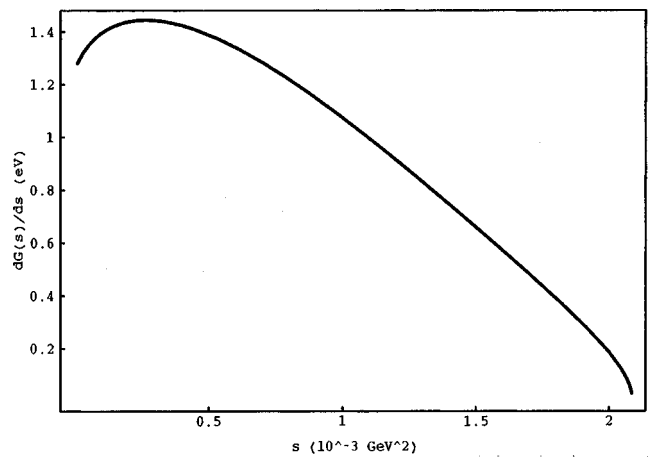


FIG. 11. The differential decay widths $d\Gamma(B^* \rightarrow B \gamma \gamma)/ds$ (eV) as a function of s , with the value $g=0.5$ and $\mu=11.0$.

appropriate tool for its measurement. For the conventionally envisaged range $0.25 < g < 1$ we calculated $1.6 \times 10^{-6} < \text{Br}(D^{*0} \rightarrow D^0 \gamma \gamma) < 3.3 \times 10^{-5}$.

On the other hand, $\text{Br}(B^{*0} \rightarrow B^0 \gamma \gamma)$ is a function of $g_{B^*B\pi}$, $g_{B^*B^0\gamma}$ and $g_{B^*B^+\gamma}$. The latter coupling has little effect on the branching ratio. Nevertheless, one cannot determine specific values for the first two couplings from the measured branching ratio, unless g is in the higher part of its expected range, say $0.6 - 1$.

The differential $d\Gamma/ds$ distributions in both cases can be used as additional help for extracting the values of the coupling constants. If the value of $g_{B^*B\pi}$ will turn out to be in

the ‘‘measurable’’ range, it will be of great interest to check the $\text{HM}\chi\text{L}$ relation $g_{B^*B\pi}/g_{D^*D\pi} = M_B/M_D$.

ACKNOWLEDGMENTS

We are in debt to Professor Gad Eilam for helpful remarks and stimulating discussions. We also acknowledge discussions with Dr. Simon Robins, Dr. Yoram Rozen, and Dr. Shlomit Terem on the feasibility of the relevant detection experiments. The research of P.S. has been supported in part by the Fund for Promotion of Research at the Technion.

-
- [1] CUSB Collaboration, K. Han *et al.*, Phys. Rev. Lett. **55**, 36 (1985).
- [2] CUSB-II Collaboration, J. Lee-Franzini *et al.*, Phys. Rev. Lett. **65**, 2947 (1990).
- [3] ALEPH Collaboration, Z. Phys. C **69**, 393 (1996); DELPHI Collaboration, *ibid.* **68**, 353 (1995); L3 Collaboration, Phys. Lett. B **345**, 589 (1995); OPAL Collaboration, Z. Phys. C **74**, 413 (1997).
- [4] Particle Data Group, C. Caso *et al.*, Euro. Phys. J. C **3**, 1 (1998).
- [5] E. Eichten *et al.*, Phys. Rev. D **21**, 203 (1980).
- [6] S. Godfrey and N. Isgur, Phys. Rev. D **32**, 189 (1985).
- [7] M. A. Ivanov and Yu. M. Valit, Z. Phys. C **67**, 633 (1995).
- [8] P. Singer and G. A. Miller, Phys. Rev. D **39**, 825 (1989).
- [9] P. Cho and H. Georgi, Phys. Lett. B **296**, 408 (1992).
- [10] J. F. Amundson *et al.*, Phys. Lett. B **296**, 415 (1992).
- [11] P. Colangelo, F. De Fazio, and G. Nardulli, Phys. Lett. B **316**, 555 (1993).
- [12] N. Barik and P. C. Dash, Phys. Rev. D **49**, 299 (1994).
- [13] P. Colangelo, F. De Fazio, and G. Nardulli, Phys. Lett. B **334**, 175 (1994).
- [14] H. G. Dosch and S. Narison, Phys. Lett. B **368**, 163 (1996).
- [15] T. M. Aliev *et al.*, Phys. Rev. D **54**, 857 (1996).
- [16] I. Peruzzi *et al.*, Phys. Rev. Lett. **37**, 569 (1976); Mark I Collaboration, G. Goldhaber *et al.*, Phys. Lett. **69B**, 503 (1977); G. J. Feldman *et al.*, Phys. Rev. Lett. **38**, 1313 (1977).
- [17] JADE Collaboration, W. Bartelt *et al.*, Phys. Lett. **161B**, 197 (1985).
- [18] HRS Collaboration, E. H. Low *et al.*, Phys. Lett. B **183**, 232 (1987); S. Abachi *et al.*, *ibid.* **212**, 533 (1988).
- [19] CLEO Collaboration, F. Butler *et al.*, Phys. Rev. Lett. **69**, 2041 (1992).
- [20] ARGUS Collaboration, H. Albrecht *et al.*, Z. Phys. C **66**, 63 (1995).
- [21] CLEO Collaboration, J. Bartelt *et al.*, Phys. Rev. Lett. **80**, 3919 (1998).
- [22] ACCMOR Collaboration, S. Barlag *et al.*, Phys. Lett. B **278**, 480 (1992).
- [23] R. L. Thews and A. N. Kamal, Phys. Rev. D **32**, 810 (1985); E. Sucipto and R. L. Thews, *ibid.* **36**, 2074 (1987).
- [24] T. N. Pham, Phys. Rev. D **25**, 2955 (1982).
- [25] P. J. O'Donnell and Q. P. Xu, Phys. Lett. B **336**, 113 (1994).
- [26] G. A. Miller and P. Singer, Phys. Rev. D **37**, 2564 (1988).
- [27] V. M. Belyaev, V. M. Braun, A. Khodjamirian, and R. Ruckl, Phys. Rev. D **51**, 6177 (1995).
- [28] A. N. Ivanov and N. I. Troitskaya, Phys. Lett. B **345**, 175 (1995).
- [29] A. N. Kamal and Q. P. Xu, Phys. Lett. B **284**, 421 (1992).
- [30] I. Stewart, Nucl. Phys. **B529**, 62 (1998).
- [31] M. B. Wise, Phys. Rev. D **45**, R2188 (1992).
- [32] G. Burdmann and J. Donoghue, Phys. Lett. B **280**, 287 (1992).
- [33] T. M. Yan *et al.*, Phys. Rev. D **46**, 1148 (1992); **55**, 5851(E) (1997).
- [34] R. Casalbuoni *et al.*, Phys. Rep. **281**, 145 (1997).
- [35] H.-Y. Cheng *et al.*, Phys. Rev. D **47**, 1030 (1993).
- [36] H.-Y. Cheng *et al.*, Phys. Rev. D **49**, 2490 (1994); **49**, 5857 (1994).
- [37] C. G. Boyd and B. Grinstein, Nucl. Phys. **B442**, 205 (1995).
- [38] A. K. Leibovich, A. V. Manohar, and M. B. Wise, Phys. Lett. B **358**, 347 (1995); **376**, 332(E) (1996).
- [39] P. Colangelo *et al.*, Phys. Lett. B **339**, 151 (1994).
- [40] A. V. Manohar and H. Georgi, Nucl. Phys. **B234**, 189 (1984).
- [41] N. Isgur and M. B. Wise, Phys. Rev. D **41**, 151 (1990).
- [42] S. Nussinov and W. Wetzel, Phys. Rev. D **36**, 130 (1987).
- [43] UKQCD Collaboration, G. M. de Divitiis *et al.*, J. High Energy Phys. **10**, 010 (1998).
- [44] D. Guetta and P. Singer (unpublished).